Electrochimica Acta 271 (2018) 417–424

Contents lists available at ScienceDirect

Electrochimica Acta

journal homepage: www.elsevier.com/locate/electacta

A novel dual-signal electrochemical sensor for bisphenol A determination by coupling nanoporous gold leaf and self-assembled cyclodextrin

Ruyue Zhang [a, 1], Yang Zhang [b, 1], Xiling Deng [a], Shiguo Sun [a], Yingchun Li [b, *]

[a] Key Laboratory of Xinjiang Phytomedicine Resource and Utilization, Ministry of Education, School of Pharmacy, Shihezi University, Shihezi, 832000, China
[b] College of Science, Harbin Institute of Technology, Shenzhen, 518055, China

ARTICLE INFO

Article history:
Received 7 January 2018
Received in revised form
19 March 2018
Accepted 19 March 2018
Available online 20 March 2018

Keywords:
Electrochemical sensor
Nanoporous gold leaf
Dual-signal strategy
Cyclodextrin
Bisphenol A

ABSTRACT

Bisphenol A (BPA) is an endocrine disrupting chemical, which can mimic estrogen and bring about a series of negative impact on human health. Herein, we developed a novel dual-signal sensor by coupling nanoporous gold leaf (NPGL) with thiolated beta-cyclodextrin (SH-β-CD) to realize sensitive and selective determination of BPA. Modification with NPGL and self-assembling of SH-β-CD on gold electrode were tracked by scanning electron microscopy, energy-dispersive spectroscopy and electrochemical measurements. The dual signaling method is based on the competitive host–guest interaction by recording the signals from both target molecule BPA and probe molecule methylene blue (MB). Due to the different binding ability of host molecule (β-CD) towards BPA and MB, BPA is able to enter β-CD cavities and replace the pre-existing MB, resulting in the decreased oxidation peak current of MB and the increased oxidation peak current of BPA. The summation of both current changes ($|\Delta I_{MB}| + \Delta I_{BPA}$) is linearly dependent on Napierian logarithm of BPA concentration from 3×10^{-7} M to 1×10^{-4} M with a detection limit of 6×10^{-8} M (S/N = 3). It is noted that the detection limit obtained by dual-signaling is much lower than that using single ΔI_{BPA} as the response signal. This newly developed sensor was further adopted to measure BPA in milk and tap water. The proposed dual-signal strategy and the established hybrid electrochemical sensor have great potential applications in biomarker detection, food safety testing and environmental monitoring.

1. Introduction

As an endocrine disrupting chemical, estrogen-mimicking Bisphenol A (BPA) can lead to a broad range of disease in animals and human beings even at a low concentration [1,2]. BPA has been added to the candidate list of substances of very high concern in several countries, where strict assessment of this substance are stipulated [3]. Many analytical techniques have been reported for BPA detection including fluorimetry [4], liquid chromatography [5], enzyme-linked immunosorbent assay [6] and electrical sensing methods [7]. Among them, electrochemical sensors have attracted wider attentions thanks to fast response speed, ease of miniaturization and easy to operate, which has advantages over large instrument-based strategies [8,9]. As electrochemical signal generated by BPA is quite weak at bare electrode, modification of electrode with suitable catalytic materials is indispensable to obtain amplified signals and enhanced selectivity and sensitivity [7].

Sensors modified with noble nano-metals, such as Au nanoparticles (AuNPs) [10,11], Au nanocluster [12,13] and nanoporous gold leaf (NPGL) [14,15], exhibit high electrical catalytic properties due to their enlarged surface area and improved electron transfer rate. Among them, NPGL is an very attractive agent with unique three-dimensional interconnected architecture, and uniformly distributed nanoligaments and nanopores [16]. Compared with AuNPs and Au nanocluster, NPGL is a free-standing thin film with continuous mesoporous structure, which ensures stability of NPGL-decorated electrodes by preventing particle aggregation and shedding [17]. In our previous work, several sensors based on NPGL have been developed with improved sensitivity, and also exhibit excellent features like easy fabrication, high repeatability and good

* Corresponding author.
E-mail address: liyingchun@hit.edu.cn (Y. Li).
[1] These authors contributed equally to this work.

https://doi.org/10.1016/j.electacta.2018.03.113
0013-4686/

stability, demonstrating that NPGL is a favorable material in sensor modification [18–20].

The dual signaling electrochemical sensing strategy combining merits of "signal-on" and "signal-off" has received much more attention on account of its good analytical performance such as low detection limit, good repeatability and low back ground noise [21–23]. Compared to traditional sensor with single signal output, electrochemical sensor with dual-signal output is promising because it can efficiently overcome potential interferences from intrinsic background electrochemical signals, which are difficult to avoid in single signal sensor system. Hence, dual-signal electrochemical sensors include an intrinsic built-in correction to the effects from system or background electric signals, and show a significant potential to further improve accuracy and sensitivity in practical applications. Several dual-signal sensors are developed utilizing cyclodextrins (CDs) as the host molecules for molecular recognition [24–26]. CDs are able to selectively retain target analytes of proper geometrical fitting in their nanocavities [27,28], depending on binding constant and binding strength between CDs and analytes [29,30]. Thanks to good molecular enrichment capability and host-guest recognition ability [31], CDs as modification material are able to improve selectivity of sensor.

Our work presented a dual-signal electrochemical sensing strategy for sensitively and selectively measuring BPA based on host-guest competitive interaction. The sensor was fabricated by coupling NPGL with self-assembled thiolated beta-cyclodextrin (SH-β-CD). The target molecules were absorbed on the electrode surface and signals changed can be recorded. Methylene blue (MB) was selected as an electrochemical signal probe, due to its strong electroactivity and the ability to form host-guest complex with CDs [32,33]. BPA can replace the pre-existing MB molecules from cavities of CDs, which results in the reduced current of MB and the increased current of BPA. Herein, integration of both current changes as dual signals was proved to improve sensitivity for BPA assay compared with single signal. This is the first report about combination of NPGL and CDs as decoration material for constructing electrochemical sensor so far. Furthermore, the hybrid sensor was employed to detect BPA in milk and tap water successfully.

2. Experimental

2.1. Materials and reagents

Au/Ag alloy leaves (40:60 wt%) with a thickness of 100 nm were obtained from Suzhou Cold Stones Tech. Co. Ltd. Mono-(6-mercapto-6-deoxy)-β-cyclodextrin (SH-β-CD) was bought from Shandong Bingzhou Zhiyuan Biotech Co. Ltd. Bisphenol A (BPA), Methylene blue (MB), diallyl bisphenol A (DBA), 4,4′-sulphonylbis (SPB) and carbamazepine (CBZ) were purchased from Adamas Reagent Co. Ltd. (Shanghai, China). All other chemicals used in this work, such as $[Fe(CN)_6]^{3-/4-}$, methanol, ethanol, KH_2PO_4, K_2HPO_4 and KCl, were obtained from Guangfu Tech. Co. Ltd. (Tianjin, China). Milk was bought from local market and tap water was obtained from the lab. All the reagents were of analytical grade or better. Water was doubly distilled. BPA was dissolved in ethanol at a concentration of 0.05 M as stock solution, which was diluted to different concentrations with 0.1 M phosphate buffer before use.

2.2. Instruments

The electrochemical measurements, such as cyclic voltammetry (CV), electrochemical impedance spectroscopy (EIS) and square wave voltammetry (SWV), were carried out on a CHI 660 E Electrochemical Workstation (ChenHua Instruments Co., Shanghai, China). A typical three-electrode system was adopted with a bare or modified gold electrode (GE, 4 mm in diameter) as the working electrode, a platinum wire as the counter electrode and a saturated calomel electrode (SCE) as the reference electrode. Scanning electron microscopy (SEM, Zeiss Supra 55VP) and energy-dispersive spectroscopy (EDS, Scanning Electron Microscope, Zeiss Supra 55VP) were applied for surface morphology characterization. UV–vis spectra were recorded on a UV-2600 UV–vis spectrophotometer (UV–vis, Shimadzu). High performance liquid chromatography (HPLC, Shimadzu) was adopted as a reference to validate the proposed approach in BPA detection. A centrifuge (Anke TGL-16G, China) was utilized to pretreat real samples.

2.3. Fabrication of sensor

The bare GE was first polished repeatedly to a mirror finish with 0.3 mm and 0.05 mm Al_2O_3, and thoroughly cleaned by ultrasonication in distilled water and ethanol for 30 s respectively. NPGL made by selective removal of Ag was similar to that in previous reports [34]. In brief, Ag/Au alloy leaf was cut into small squares, and then immerged in concentrated nitric acid (65 vol%) for 60 min. Subsequently, the leaf was washed repeatedly with distilled water and carefully transferred onto GE surface by following our previous reports [18]. Then the NPGL-modified GE (NPGL/GE) was dried at room temperature. NPGL/GE was pretreated with CV scanning from −0.3 V to 1.5 V at a scan rate of 50 mV s^{-1} for 24 cycles in 0.5 M H_2SO_4 aqueous solution to get a clean electrode. After that, the NPGL/GE was thoroughly washed with water and soaked in aqueous solution of SH-β-CD (1 mg mL^{-1}) for about 15 h at 4 °C. The electrode was marked as SH-β-CD/NPGL/GE and rinsed again with ethanol and water before electrochemical measurement. All the sensors were stored at 4 °C when not in use.

2.4. Electrochemical measurement

EIS and SWV are conducted to characterize differently modified electrodes. EIS experiment was operated in an aqueous solution containing 5 mM $[Fe(CN)_6]^{3-/4-}$ and 0.1 M KCl. SWV was carried out in a potential range of −0.5 to +0.8 V in phosphate buffer (pH 7.0, 0.1 M). In particular, before electrochemical determination of BPA via SWV, the SH-β-CD/NPGL/GE was first incubated with MB (50 μM, 10 mL) aqueous solution, gently rinsed with distilled water, and then underwent the second round of incubation in BPA solution.

2.5. Real sample pretreatment

To explore its practical application, the fabricated sensor was adopted to determine BPA in tap water and milk. Briefly, tap water was mixed with methanol at a volume ratio of 1:4, and then a set number of BPA was added, followed by centrifugation at 4000 rpm for 5 min. As for milk sample preparation, milk containing a certain amount of BPA was mixed with methanol at a volume ratio of 1:4. The mixture was centrifugated for 10 min at 4000 rpm to remove protein. The obtained supernatants were used for analysis and stored at 4 °C.

3. Results and discussion

3.1. Characterization and preparation of the SH-β-CD/NPGL/GE

The fabrication process is to couple dealloying with self-assembly, and the process was monitored by SEM, EDS and electrochemical methods. As shown in Fig. 1A, the surface morphology of NPGL/GE is sponge-like with a randomly uniform porous

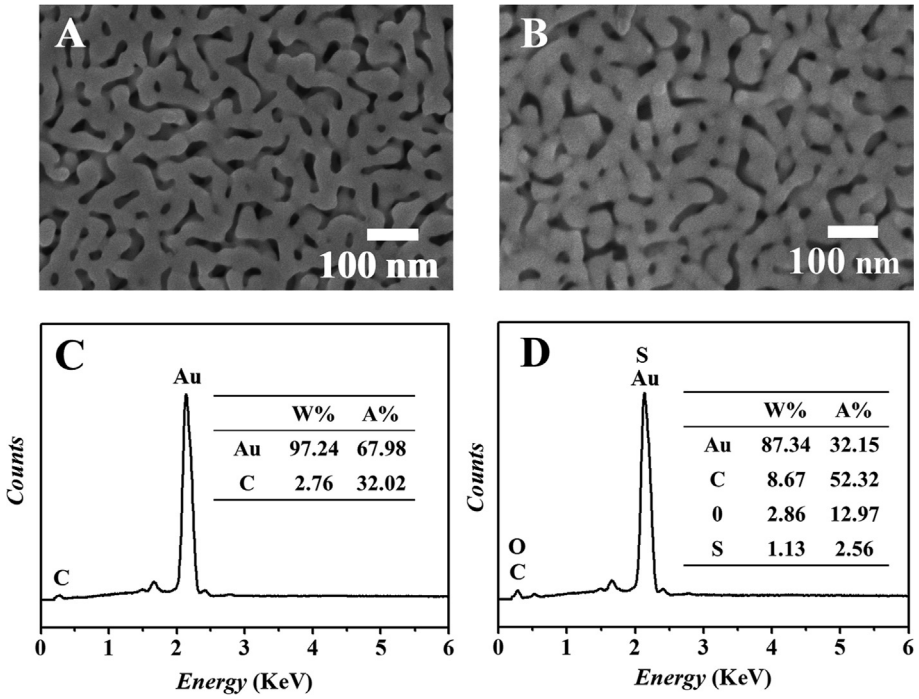

Fig. 1. SEM images of (A) NPGL/GE and (B) SH-β-CD/NPGL/GE; EDS spectra of (C) NPGL/GE and (D) SH-β-CD/NPGL/GE.

structure. After immobilization of SH-β-CD, slight reduction of the width of the nanopores can be observed (Fig. 1B), implying coverage of thin film. The direct elemental content information was collected by EDS, and the corresponding spectra were shown in Fig. 1C–D. As expected, sulfur and oxygen elements appear in SH-β-CD/NPGL/GE. Both experiments confirm that SH-β-CD was successfully assembled onto the surface of NPGL/GE.

To further explore interface property, EIS was applied to investigate stepwise sensor construction process. The results of differently modified electrodes (bare GE, NPGL/GE, SH-β-CD/GE and SH-β-CD/NPGL/GE) in 5.0 mM $[Fe(CN)_6]^{3-/4-}$ aqueous solution containing 0.1 M KCl were shown in Fig. 2A. Bare GE had a relatively low charge-transfer resistance (R_{ct}) with a small semicircle domain ($R_{ct} = 185.34\ \Omega$), whereas NPGL/GE showed almost a straight line with R_{ct} of 22.53 Ω, indicating a very fast charge-transfer process due to excellent electronic transmission capability of NPGL. In contrast, after assembly of SH-β-CD molecules on GE, the electrode generated higher interfacial resistance with R_{ct} of 825.76 Ω. After assembling SH-β-CD on NPGL/GE, R_{ct} of the electrode increased to 374.96 Ω, as the consequence of the balanced influence of NPGL and SH-β-CD [35].

The electrochemical behavior of BPA on differently modified electrode was studied via SWV in 0.1 M phosphate buffer (pH 7.0) after incubation in BPA (50 μM) for 30 min. As displayed in Fig. 2B, a weak oxidation peak current of BPA was obtained at bare GE. However, when SH-β-CD assembled on the surface of GE, the modified electrode presents a enhanced peak current, which probably results from the high affinity of SH-β-CD to BPA. After NPGL coating, the current of BPA at NPGL/GE slightly increased in comparison with that of bare GE, probably due to the relative poor enrichment ability of NPGL/GE toward BPA. The largest peak currents were obtained at SH-β-CD/NPGL/GE because of the synergetic effect of NPGL and SH-β-CD, where the former provides large surface area and fast electron transmission, and the latter possesses good molecular enrichment capability and host-guest recognition ability.

3.2. Feasibility of the SH-β-CD/NPGL/GE

Spectrophotometric experiments were adopted to demonstrate formation of inclusion complexes between guest (MB or BPA) and host (SH-β-CD) molecules [36]. The UV–vis spectra of MB (5 μM) and BPA (10 μM) in the absence and presence of SH-β-CD (100 μM) in aqueous solution were recorded. As displayed in Fig. 2C, after addition of SH-β-CD, UV absorption intensities of BPA and MB increased while their absorption bands remained unchanged. This might arise from solubility elevation of BPA and MB in water as the result of SH-β-CD introduction, implying formation of host-guest inclusion complex.

To prove competing event of the constructed system, SH-β-CD/NPGL/GE was separately incubated in 50 μM MB, in 50 μM BPA or first in MB followed by BPA solutions. Each incubation time took 20 min, and afterwards SWV spectra of the electrodes were recorded in 0.1 M phosphate buffer (pH 7.0). The electrooxidation peak potentials of MB and BPA are −0.28 V and 0.57 V, respectively (Fig. 2D). When SH-β-CD/NPGL/GE was first incubated with MB and then underwent the second round of incubation in BPA, competitive association of BPA and MB to SH-β-CD occurs. The current of MB in curve c decreased evidently compared with that in curve a, while the current of BPA was almost the same as that in curve b, suggesting that the binding between SH-β-CD and BPA is greater than that between SH-β-CD and MB. This phenomenon further indicates that, although SH-β-CD cavities are occupied by MB in advance, BPA is still able to enter the cavities, replace MB molecules and form inclusion complex with SH-β-CD. Therefore, the boosting peak current of BPA and reduction of MB can be combined as a dual-signal sensing strategy for BPA analysis (Fig. 3).

3.3. Experimental conditions optimization

Six experimental conditions were optimized during sensor preparation, which included concentration of SH-β-CD, self-assembly time of SH-β-CD, pH of supporting electrolyte,

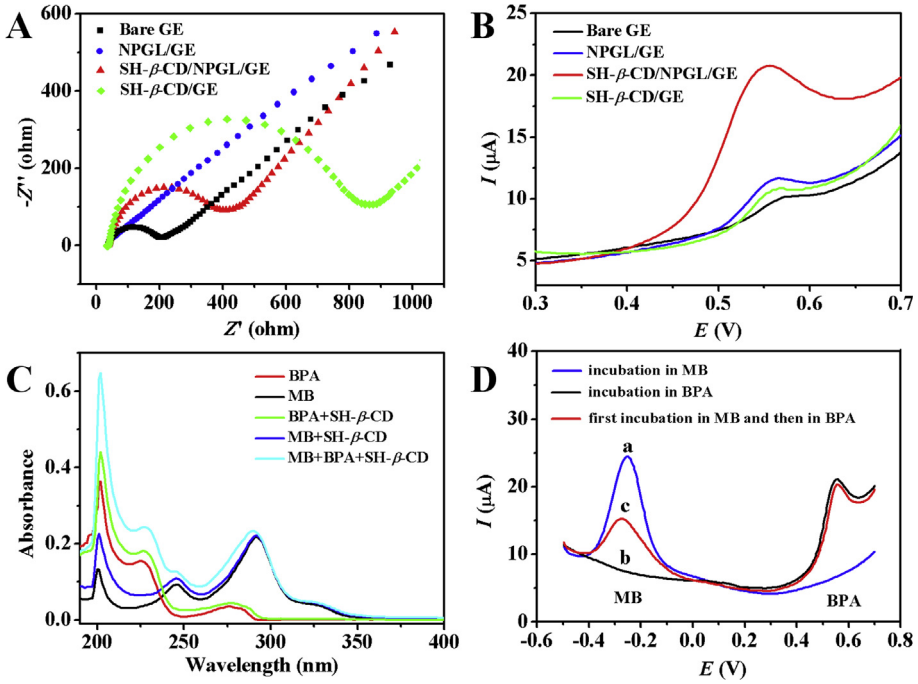

Fig. 2. (A) EIS at bare GE, NPGL/GE, SH-β-CD/GE and SH-β-CD/NPGL/GE in 5 mM $[Fe(CN)_6]^{3-/4-}$ and 0.1 M KCl. The frequency range of EIS was from 0.01 Hz to 100 kHz. (B) SWV plots at bare GE, NPGL/GE, SH-β-CD/GE and SH-β-CD/NPGL/GE for determination of 50 μM BPA in 0.1 M phosphate buffer (pH 7.0). (C) UV–vis spectra of inclusion complex: 10 μM BPA, 5 μM MB, 100 μM SH-β-CD, mixture of 10 μM BPA and 100 μM SH-β-CD, and mixture of 5 μM MB and 100 μM SH-β-CD. (D) SWV responses of SH-β-CD/NPGL/GE in phosphate buffer (0.1 M, pH 7.0) after incubated in 50 μM MB, 50 μM BPA, and first in 50 μM MB and then in 50 μM BPA.

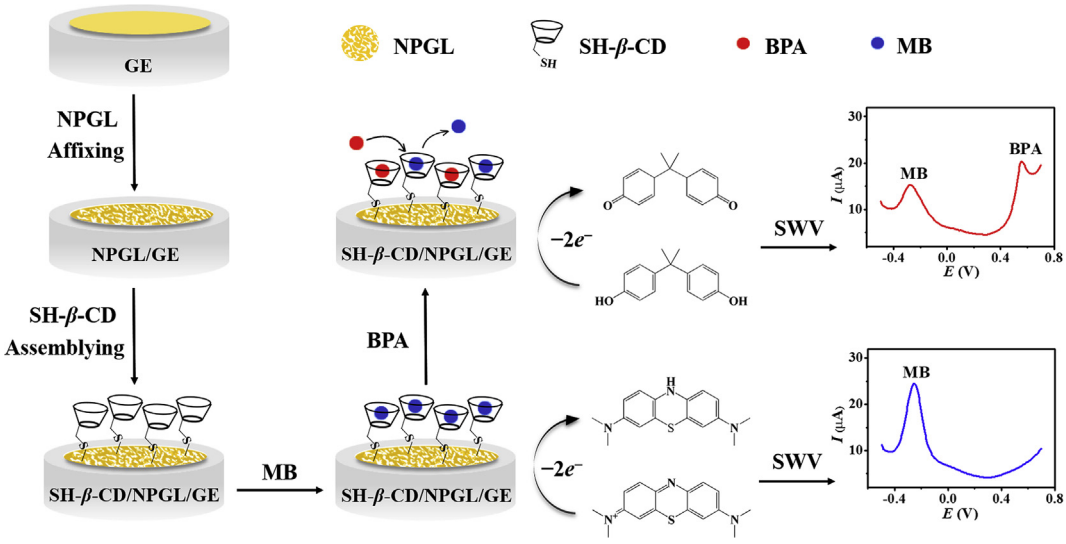

Fig. 3. Schematic representation of SH-β-CD/NPGL/GE fabrication and electrochemical detection of BPA.

incubation concentration and time of MB, and incubation time of BPA. All the differently prepared sensors were investigated via SWV in 0.1 M phosphate buffer.

Concentration and assembling time of SH-β-CD during self-assembly were evaluated via exploring the sensor response toward 50 μM BPA in phosphate buffer at pH 7.0. As showed in Fig. 4A, the peak current of BPA increased with raising the concentration of SH-β-CD from 0.1 mg mL^{-1} to 1.0 mg mL^{-1}, and then decreased slightly when the concentration exceeds 1.0 mg mL^{-1}. This is probably owing to the fact that the amount of SH-β-CD molecules on NPGL/GE reaches its maximum. In Fig. 4B, it shows impact of self-assembly time of SH-β-CD in the range of 10–24 h. It is noted that the response of BPA rose to maximum at 15 h and then went down. Briefly, with the increase of assembly time, the amount of SH-β-CD bound at NPGL/GE increased gradually, and therefore more BPA molecules were enriched, leading to increased oxidation peak current. However, as the assembly time goes by, the amount of SH-β-CD at NPGL/GE surface reaches saturation, so the current response of the BPA no longer changes. Therefore, 15 h was chosen as the optimal duration, since it allows the constructed sensor providing sufficient cavities for BPA binding without affecting electron transfer.

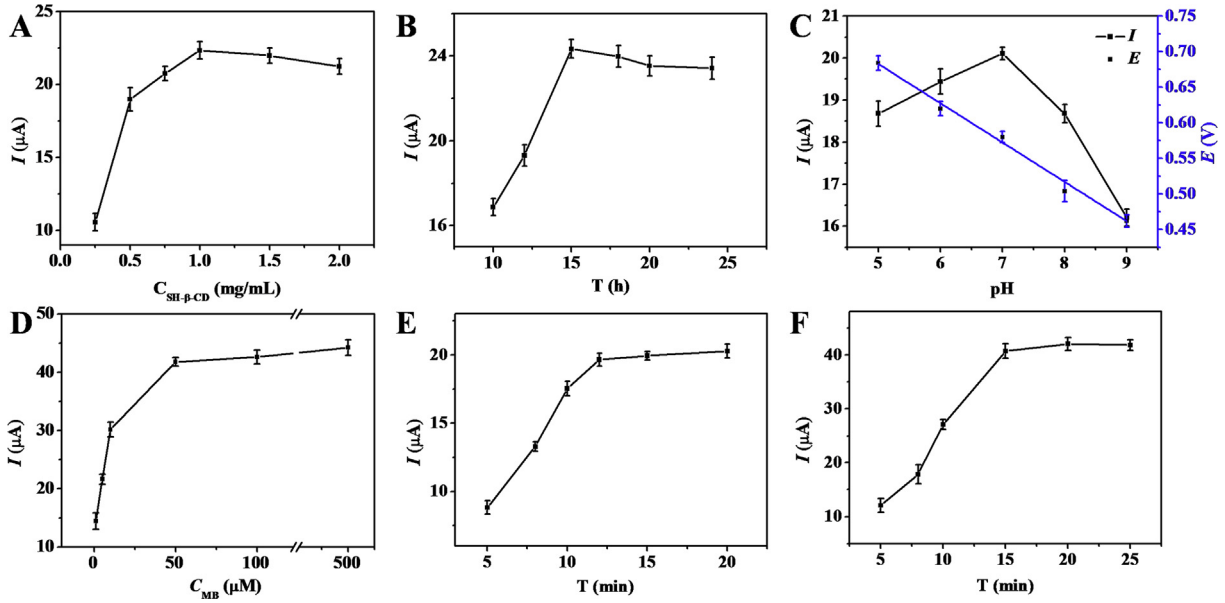

Fig. 4. Effect of (A) SH-β-CD concentration, (B) self-assembly time, (C) pH of supporting electrolyte on peak current of BPA oxidation. Effect of (D) incubation concentration and (E) incubation time of MB on peak current of MB oxidation. Effect of (F) incubation time of BPA on peak current of BPA oxidation.

Effect of solution pH was studied by testing the response of 50 μM BPA. In Fig. 4C, the peak current of BPA first increased and then reduced with increasing pH and the maximum response for BPA was obtained at pH 7.0, indicating that protons are associated with oxidation reaction of BPA. It is known that the existence form of solute can be affected by pH of solution, and when pH is smaller than pKa, solute will be mainly present in non-dissociated status. Herein, pKa value of BPA is 9.73 [9]; hence, when pH is around 7.0, most of BPA molecules are non-dissociated. Compared with dissociated BPA, the non-dissociated ones own larger tendency to be absorbed on electrode surface, thereby leading to a higher sensing response. It is also found that the oxidation peak potential of BPA was negatively shifted as pH value increased. The change between peak potential and pH value shows a good linear relationship and the equation is: E_{pa} (V) = 0.962−0.056 pH (R^2 = 0.9919). The slope of 56 mV pH^{-1} is close to the theoretical value of 57.6 mV pH^{-1} [37], suggesting that equal numbers of electrons and protons were involved in charge transfer. Considering the sensitivity of BPA assay, the pH of supporting electrolyte was set to be 7.0.

The effect of incubation concentration of MB was investigated by checking SWV peak current of MB-incubated SH-β-CD/NPGL/GE in phosphate buffer at pH 7.0. Responses were recorded after sensor was soaked in MB solution at different concentrations for 1 h. As shown in Fig. 4D, the response increased with the increased concentration. Plateau was reached at 50 μM, implying that cavities of SH-β-CD were fully accommodated by MB molecules at this point. Therefore, 50 μM was selected as the optimal concentration for MB incubation solution.

The incubation time of MB and BPA is also vital for sensing performance, which was explored in 0.1 M phosphate buffer (pH 7.0) after sensor was soaked in MB (50 μM) or BPA (50 μM) for different periods of time. As showed in Fig. 4E–F, current of electrode increased with the increase of incubation time, maximum values were attained at 12 min for BPA and 15 min for MB, which were adopted for the following experiments.

3.4. Calibration curve

Under the optimal experimental conditions, dual-signal strategy for quantitative detection of BPA was carried out by using MB-incubated SH-β-CD/NPGL/GE via SWV. As displayed in Fig. 5A, it is observed that oxidation peak current of MB decreases while that of BPA increases with increasing BPA concentration. The summation of both current changes ($|\Delta I_{MB}| + \Delta I_{BPA}$) is linearly dependent on Napierian logarithm of BPA concentration from 3×10^{-7} M to 1×10^{-4} M (Fig. 5B) and the corresponding linear equation is $|\Delta I_{MB}| + \Delta I_{BPA}$ (μA) = 14.928 LgC + 13.589 (R^2 = 0.9928). The limit of detection (LOD) was measured and calculated to be 6×10^{-8} M based on signal-to-noise of 3 (S/N = 3). Moreover, the comparison of our senor with other reported electrochemical sensors for BPA analysis is summarized in Table 1. It is found that our SH-β-CD/NPGL/GE exhibits the lowest LOD and wider linear range compared with the previous reports. The good performance could be attributed to the combined advantages of molecular recognition ability of SH-β-CD and the dual-signaling strategy.

As a comparison to the above-mentioned dual-signal method, single BPA signal was record for establishing the quantitative relationship. The calibration curve of the change value of BPA oxidation peak current (ΔI_{BPA}) versus Napierian logarithm of BPA concentration was got in the range of 5×10^{-7}–5×10^{-6} M with a LOD of 2.6×10^{-7} M (S/N = 3) (Fig. 5B), and the corresponding linear equation is ΔI_{BPA} (μA) = 6.2664 LgC + 3.0371 (R^2 = 0.9944). It is worth mentioning that the LOD obtained by dual-signal approach ($|\Delta I_{MB}| + \Delta I_{BPA}$ as response signal) is much lower than that of single signal strategy (ΔI_{BPA} as response signal). And the sensitivity for BPA determination by using dual signaling is 4.80 μA/μM while that of single signaling method is 1.48 μA/μM.

3.5. Selectivity, repeatability, reproducibility and stability of SH-β-CD/NPGL/GE

Structural analogues of BPA, including DBA, SPB and CBZ, were used as potentially interference substances to test the selectivity of SH-β-CD/NPGL/GE. It was found that current response of BPA was much higher than the three interfering substances at the same

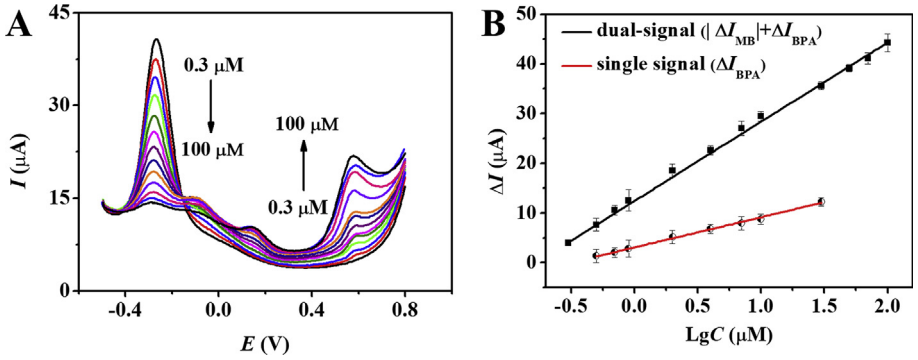

Fig. 5. (A) SWV responses of the MB-incubated SH-β-CD/NPGL/GE in phosphate buffer (0.1 M, pH 7.0) after incubation with BPA in the concentration range of 3×10^{-7}–1×10^{-4} M. (B) Calibration curve for BPA detection correlating oxidation peak current shift (Δ*I*) with the Napierian logarithm of BPA concentration by using SH-β-CD/NPGL/GE. The measurements were carried out for 3 times.

Table 1
Comparison of the major characteristics of some reported electrochemical methods for BPA determination.

Electrodes	Methods	Dynamic range (M)	LOD (M)	References
Thionine/CB[a]/SPE[b]	Amperometry	5.0×10^{-7}–5.0×10^{-5}	2.0×10^{-7}	[38]
MWCNTs[c]/Au/paper electrode	Linear sweep voltammetry	7.0×10^{-7}–7.0×10^{-5}	1.0×10^{-7}	[39]
CYP2C9–PAM[d] film electrodes	Amperometry	1.2×10^{-6}–1.0×10^{-5}	5.8×10^{-7}	[40]
BDD[e] electrode	Differential pulse voltammetry	4.4×10^{-7}–5.2×10^{-6}	7.1×10^{-7}	[41]
CNTPE[f]	Linear sweep voltammetry	1.0×10^{-6}–4.0×10^{-6}	0.7×10^{-7}	[42]
$[Ru(bpy)_3]^{2+}$/ITO[g]	Differential pulse voltammetry	5.0×10^{-6}–1.2×10^{-4}	2.9×10^{-7}	[43]
AuNp[h]@MOF[i]/CPE[j]	Differential pulse voltammetry	2.0×10^{-4}–1.0×10^{-3}	3.7×10^{-6}	[44]
SH-β-CD/NPGL/GE	SWV	3.0×10^{-7}–1.0×10^{-4}	6.0×10^{-8}	This work

[a] CB: carbon black.
[b] SPE: screen printed electrode.
[c] MWCNTs: multi-walled carbon nanotubes.
[d] PAM: polyacrylamide.
[e] BDD: boron-doped diamond.
[f] CNTPE: multiwall carbon nanotubes paste electrode.
[g] ITO: indium-tin oxide.
[h] AuNp: gold nanoparticles.
[i] MOF:metal organic framework.
[j] CPE: carbon paste electrode.

concentration (Fig. 6A). In addition, some ions possibly existing in real samples like NH_4^+, K^+, Na^+, NO_3^-, Cl^- and SO_4^{2-}, were examined using the developed method with a concentration 10-fold higher than that of BPA. The current response difference between BPA alone and the BPA and ions mixture was 94.6%, suggesting remarkable anti-interference capability of the sensor.

To evaluate repeatability, one MB-incubated SH-β-CD/NPGL/GE was used for electrochemical detection of 50 μM BPA for ten continuous times, and the relative standard deviation (RSD) was less than 2.8%. As for reproducibility, five different sensors were manufactured independently by the same approach, and RSD of sensor response to BPA was 5.7%. Furthermore, the modified electrode was stored at 4 °C for 2 weeks, and a response decrease by 10.2% was observed, which is acceptable for practical application. Further work is in progress to enhance the sensor's long-term stability.

3.6. Real sample analysis

To further explore reliability of the sensor, recovery of different

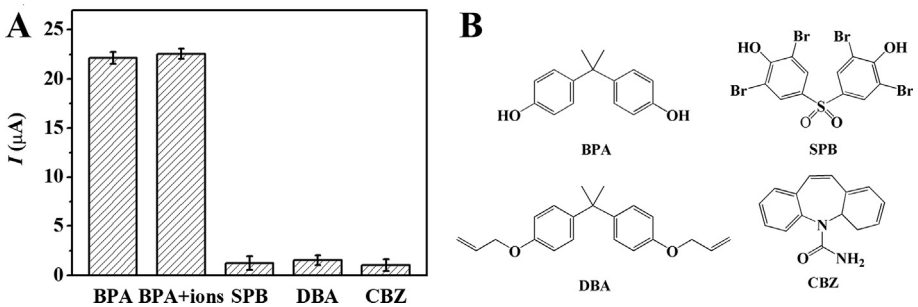

Fig. 6. (A) Sensor responses towards BPA, the mixtures of BPA and interfering ions (NH_4^+, K^+, Na^+, NO_3^-, Cl^- and SO_4^{2-}), and structural analogues of BPA using SH-β-CD/NPGL/GE. (B) Chemical structures of BPA and its structural analogues. The concentration of BPA and its structural analogues is 50 μM, and concentration of co-existing ions is 10-fold higher than that of BPA.

Table 2
Determination of BPA in real sample using SH-β-CD/NPGL/GE and HPLC (n = 3)[a,b].

Method	Sample	Determined	Spiked[c]	Total found[c]	Recovery (%)	RSD (%)
SH-β-CD/NPGL/GE	Tap water	–	3.0	2.92 ± 0.0785	97.3	2.7
		_	4.0	4.12 ± 0.1043	103.0	2.5
		_	5.0	5.09 ± 0.1584	101.8	3.1
	Milk	–	3.0	3.16 ± 0.1192	105.3	3.8
		_	4.0	3.99 ± 0.0822	99.7	2.1
		_	5.0	5.18 ± 0.2754	103.6	5.3
HPLC	Tap water	–	3.0	2.97 ± 0.0159	99.0	0.5
		_	4.0	3.89 ± 0.0310	97.2	0.8
		_	5.0	5.03 ± 0.0149	100.6	0.3
	Milk	–	3.0	3.08 ± 0.0372	102.6	1.2
		_	4.0	3.99 ± 0.0452	99.7	1.1
		_	5.0	5.09 ± 0.0353	101.2	0.7

[a] Mean value ± S.D.
[b] –: Not detected.
[c] The units of the value is 10^{-5} M for HPLC and SH-β-CD/NPGL/GE.

concentrations of BPA in tap water and milk samples was detected using standard addition method. The recoveries varying from 97.3% to 103.0% for tap water and 99.7%to105.3% for milk samples were showed in Table 2, indicating that SH-β-CD/NPGL/GE exhibits satisfying accuracy for BPA detection in real samples. In addition, HPLC as a stand method was applied to analyze the same samples, whose results illustrate a superb accordance with the data obtained by our developed methodology, implying good accuracy and reliability of the proposed sensor.

4. Conclusion

A novel dual-signaling strategy has been developed for BPA detection, by taking advantage of NPGL and β-CD. To our knowledge, this is the first report about combination of NPGL with CDs and adoption of the hybrid for electrochemical sensing. Thanks to the unique nanoporous architecture of NPGL and the decent molecular recognition ability of β-CD, the proposed sensor shows high sensitivity and selectivity for BPA determination. A wide linger range (3×10^{-7} M to 1×10^{-4} M) and a low detection limit (6×10^{-8} M) were obtained as the consequence of the synergistic effect of NPGL and β-CD. Moreover, the composite-modified sensor exhibits promising performance in analyzing real samples, and the accuracy of results is validated by the gold standard method HPLC. It should also be mentioned that the manufacture of sensor is facile and highly controllable, which benefits cost efficiency and reproducibility. Therefore, it can be fairly concluded that the proposed sensor has very promising broad range applications like biomarker detection, food testing and environmental monitoring.

Acknowledgments

The project financially supported by National Natural Science Foundation of China (81773680, 81460543) and Natural Science Foundation of Shenzhen City (JCYJ20170307150444573).

References

[1] A.V. Krishnan, P. Stathis, S.F. Permuth, L. Tokes, D. Feldman, Bisphenol-A: an estrogenic substance is released from polycarbonate flasks during autoclaving, Endocrinology 132 (1993) 2279–2286.
[2] L.N. Vandenberg, R. Hauser, M. Marcus, N. Olea, W.V. Welshons, Human exposure to bisphenol A (BPA), Reprod. Toxicol. 24 (2007) 139–177.
[3] C.A. Staples, P.B. Dome, G.M. Klecka, S.T. Oblock, L.R. Harris, A review of the environmental fate, effects, and exposures of bisphenol A, Chemosphere 36 (1998) 2149–2173.
[4] A. Ballesteros-Gómez, F.J. Ruiz, S. Rubio, D. Pérez-Bendito, Determination of bisphenols A and F and their diglycidyl ethers in wastewater and river water by coacervative extraction and liquid chromatography-fluorimetry, Anal. Chim. Acta 603 (2007) 51–59.
[5] R. Jorge, W. Thomas, Determination of bisphenols in beverages by mixed-mode solid-phase extraction and liquid chromatography coupled to tandem mass spectrometry, J. Chromatogr. A 1422 (2015) 230–238.
[6] W. Miao, B. Wei, R. Yang, C. Wu, D. Lou, W. Jiang, Z. Zhou, Highly specific and sensitive detection of bisphenol A in water samples using an enzyme-linked immunosorbent assay employing a novel synthetic antigen, New J. Chem. 38 (2014) 669–675.
[7] H. Yin, Y. Zhou, S. Ai, Q. Chen, X. Zhu, X. Liu, L. Zhou, Sensitivity and selectivity determination of BPA in real water samples using PAMAM dendrimer and CoTe quantum dots modified glassy carbon electrode, J. Hazard Mater. 174 (2010) 236–243.
[8] C. Yu, L. Gou, X. Zhou, N. Bao, H. Gu, Chitosan–Fe_3O_4 nanocomposite based electrochemical sensors for the determination of bisphenol A, Electrochim. Acta 56 (2011) 9056–9063.
[9] H. Fan, Y. Li, D. Wu, H. Ma, K. Mao, D. Fan, B. Du, H. Li, Q. Wei, Electrochemical bisphenol A sensor based on N-doped graphene sheets, Anal. Chim. Acta 711 (2012) 24–28.
[10] N. Wang, M. Lin, H. Dai, H. Ma, Functionalized gold nanoparticles/reduced graphene oxide nanocomposites for ultrasensitive electrochemical sensing of mercury ions based on thymine–mercury–thymine structure, Biosens. Bioelectron. 79 (2016) 320–326.
[11] M. Xu, Y. Song, Y. Ye, C. Gong, Y. Shen, L. Wang, L. Wang, A novel flexible electrochemical glucose sensor based on gold nanoparticles/polyaniline arrays/carbon cloth electrode, Sensor. Actuator. B Chem. 252 (2017) 1187–1193.
[12] W. Wang, T. Bao, X. Zeng, H. Xiong, W. Wen, X. Zhang, W. Sheng, Ultrasensitive electrochemical DNA biosensor based on functionalized gold clusters/graphene nanohybrids coupling with exonuclease III-aided cascade target recycling, Biosens. Bioelectron. 91 (2017) 183–189.
[13] R. Wen, H. Li, B. Chen, L. Wang, Facile preparation of fluorescent gold nanocluster via polysaccharide-templated approach and its application for Cu^{2+} sensing, Sensor. Actuator. B Chem. 248 (2017) 63–70.
[14] M. Zheng, P. Li, C. Yang, H. Zhu, Y. Chen, Y. Tang, Y. Zhou, T. Lu, Ferric ion immobilized on three-dimensional nanoporous gold films modified with self-assembled monolayers for electrochemical detection of hydrogen peroxide, Analyst 137 (2012) 1182–1189.
[15] L. Lu, X. Huang, Y. Dong, Y. Huang, X. Pan, X. Wang, M. Feng, Y. Luo, D. Fang, Facile method for fabrication of self-supporting nanoporous gold electrodes via cyclic voltammetry in ethylene glycol, and their application to the electrooxidative determination of catechol, Microchim. Acta 182 (2015) 1509–1517.
[16] S. Park, H.C. Kim, T.D. Chung, Electrochemical analysis based on nanoporous structures, Analyst 137 (2012) 3891–3903.
[17] F. Meng, X. Yan, J. Liu, J. Gu, Z. Zou, Nanoporous gold as non-enzymatic sensor for hydrogen peroxide, Electrochim. Acta 56 (2011) 4657–4662.
[18] Y. Li, J. Liu, F. Yu, H. Tang, F. Zhao, B.C. Ye, W. Chen, X. Lv, Electrochemical determination of trace lead(II) with enhanced sensitivity and selectivity by three-dimensional nanoporous gold leaf and self-assembled homocysteine monolayer, J. Electroanal. Chem. 758 (2015) 78–84.
[19] Y. Li, Y. Liu, J. Liu, J. Liu, H. Tang, C. Cao, D. Zhao, Y. Ding, Molecularly imprinted polymer decorated nanoporous gold for highly selective and sensitive electrochemical sensors, Sci. Rep-UK. 5 (2015) 7699.
[20] Y.C. Li, L. Zhang, J. Liu, S.F. Zhou, K.A. Al-Ghanem, S. Mahboob, B. Ye, X. Zhang, A novel sensitive and selective electrochemical sensor based on molecularly imprinted polymer at nanoporous gold leaf modified electrode for warfarin sodium determination, RSC Adv. 6 (2016) 43724–43731.

[21] Y.-J. Li, M.-J. Ma, J.-J. Zhu, Dual-signal amplification strategy for ultrasensitive photoelectrochemical immunosensing of α-fetoprotein, Anal. Chem. 84 (2012) 10492–10499.
[22] E. Xiong, L. Wu, J. Zhou, P. Yu, X. Zhang, J. Chen, A ratiometric electrochemical biosensor for sensitive detection of Hg^{2+} based on thymine–Hg^{2+}–thymine structure, Anal. Chim. Acta 853 (2015) 242–248.
[23] J. Zhou, X. Zhang, E. Xiong, P. Yu, X. Li, J. Chen, SDR-recycling signal amplification for highly sensitive methyltransferase activity assay, J. Electroanal. Chem. 781 (2016) 304–309.
[24] G. Zhu, L. Wu, X. Zhang, W. Liu, X. Zhang, J. Chen, A new dual-signalling electrochemical sensing strategy based on competitive host-guest interaction of a β-Cyclodextrin/Poly(N-acetylaniline)/Graphene-Modified electrode: sensitive electrochemical determination of organic pollutants, Chem. Eur J. 19 (2013) 6368–6373.
[25] P. Yu, X. Zhang, E. Xiong, J. Zhou, X. Li, J. Chen, A label-free and cascaded dual-signaling amplified electrochemical aptasensing platform for sensitive prion assay, Biosens. Bioelectron. 85 (2016) 471–478.
[26] X. Li, J. Li, Y. Liu, X. Zhang, J. Chen, A sensitive electrochemical immunosensor for prion detection based on poly- β-cyclodextrin/gold nanoparticles/glassy carbon electrode, Sensor. Actuator. B Chem. 250 (2017) 1–7.
[27] L. Wang, J. Lei, R. Ma, H. Ju, Host–guest interaction of adamantine with a β-cyclodextrin-functionalized AuPd bimetallic nanoprobe for ultrasensitive electrochemical immunoassay of small molecules, Anal. Chem. 85 (2013) 6505–6510.
[28] L. Yang, H. Zhao, C.-P. Li, S. Fan, B. Li, Dual β-cyclodextrin functionalized Au@SiC nanohybrids for the electrochemical determination of tadalafil in the presence of acetonitrile, Biosens. Bioelectron. 64 (2015) 126–130.
[29] X. Wang, H. Zeng, L. Zhao, J.M. Lin, Selective determination of bisphenol A (BPA) in water by a reversible fluorescence sensor using pyrene/dimethyl β-cyclodextrin complex, Anal. Chim. Acta 556 (2006) 313–318.
[30] A.Z.M. Badruddoza, G.S.S. Hazel, K. Hidajat, M.S. Uddin, Synthesis of carboxymethyl-β-cyclodextrin conjugated magnetic nano-adsorbent for removal of methylene blue, Colloids Surf., A 367 (2010) 85–95.
[31] K. Hamasaki, S. Usui, H. Ikeda, T. Ikeda, A. Ueno, Dansyl-modified cyclodextrins as fluorescent chemosensors for molecular recognition, Supramol. Chem. 8 (1997) 125–135.
[32] L.E. Korshoj, A.J. Zaitouna, R.Y. Lai, Methylene blue-mediated electrocatalytic detection of hexavalent chromium, Anal. Chem. 87 (2015) 2560–2564.
[33] G.C. Zhao, J.J. Zhu, H.Y. Chen, Spectroscopic studies of the interactive model of methylene blue with DNA by means of β-cyclodextrin, Spectrochim. Acta A 55 (1999) 1109–1117.
[34] L. Zhang, Y. Liu, H. Song, B. Huang, B.C. Ye, Y.C. Li, Nanoporous gold leaf as signal amplification agent for detection of VOCs with quartz crystal microbalance, Analyst 141 (2016) 4625–4631.
[35] J.L. He, Y. Yang, X. Yang, Y.L. Liu, Z.H. Liu, G.L. Shen, R.Q. Yu, β-Cyclodextrin incorporated carbon nanotube-modified electrode as an electrochemical sensor for rutin, Sensor. Actuator. B Chem. 114 (2006) 94–100.
[36] X. Kan, T. Zhang, M. Zhong, X. Lu, CD/AuNPs/MWCNTs based electrochemical sensor for quercetin dual-signal detection, Biosens. Bioelectron. 77 (2016) 638–643.
[37] L. Zhu, Y. Cao, G. Cao, Electrochemical sensor based on magnetic molecularly imprinted nanoparticles at surfactant modified magnetic electrode for determination of bisphenol A, Biosens. Bioelectron. 54 (2014) 258–261.
[38] M. Portaccio, D. Di Tuoro, F. Arduini, D. Moscone, M. Cammarota, D.G. Mita, M. Lepore, Laccase biosensor based on screen-printed electrode modified with thionine–carbon black nanocomposite, for Bisphenol A detection, Electrochim. Acta 109 (2013) 340–347.
[39] H. Li, W. Wang, Q. Lv, G. Xi, H. Bai, Q. Zhang, Disposable paper-based electrochemical sensor based on stacked gold nanoparticles supported carbon nanotubes for the determination of bisphenol A, Electrochem. Commun. 68 (2016) 104–107.
[40] P. Sun, Y. Wu, An amperometric biosensor based on human cytochrome P450 2C9 in polyacrylamide hydrogel films for bisphenol A determination, Sensor. Actuator. B Chem. 178 (2013) 113–118.
[41] G.F. Pereira, L.S. Andrade, R.C. Rocha-Filho, N. Bocchi, S.R. Biaggio, Electrochemical determination of bisphenol A using a boron-doped diamond electrode, Electrochim. Acta 82 (2012) 3–8.
[42] A. Ghanam, A.A. Lahcen, A. Amine, Electroanalytical determination of Bisphenol A: investigation of electrode surface fouling using various carbon materials, J. Electroanal. Chem. 789 (2017) 58–66.
[43] Q. Li, H. Li, G.-F. Du, Z.-H. Xu, Electrochemical detection of bisphenol A mediated by $[Ru(bpy)3]^{2+}$ on an ITO electrode, J. Hazard Mater. 180 (2010) 703–709.
[44] C.T.P. da Silva, F.R. Veregue, L.W. Aguiar, J.G. Meneguin, M.P. Moisés, S.L. Fávaro, E. Radovanovic, E.M. Girotto, A.W. Rinaldi, AuNp@MOF composite as electrochemical material for determination of bisphenol A and its oxidation behavior study, New J. Chem. 40 (2016) 8872–8877.